The Monte Carlo Method: Versatility Unbounded in a Dynamic Computing World
Chattanooga, Tennessee, April 17-21, 2005, on CD-ROM, American Nuclear Society, LaGrange Park, IL (2005)

MONTE CARLO CALCULATED RESPONSE OF THE PRM-WC2 WELL-TYPE IONIZATION CHAMBER

Tim D. Bohm and Larry A. DeWerd
Department of Medical Physics
University of Wisconsin-Madison
1300 University Ave
Madison, WI 53706 tdbohm@wisc.edu; ladewerd@wisc.edu

ABSTRACT

Permanent implantation of low energy (20-40 keV) photon emitting radioactive seeds is an important treatment option for prostate cancer patients. In order to provide effective treatments, the determination of the air kerma strength (source strength) of a radioactive seed is necessary for effective treatment planning. Typically, well-type ionization chambers having calibrations traceable to national standards are used on site at therapy clinics to independently determine the air kerma strength of seeds for quality assurance practices. Recently, we have shown that the standard temperature-pressure correction used to account for changes in the response of ion chambers open to atmospheric communication does not adequately describe the change in chamber response for low energy photon sources. This is particularly evident when the chamber is used at higher elevations where the air pressure is substantially less than that at sea level. This work will focus on examining the response of the Precision Radiation Measurements model WC2 chamber, using Monte Carlo transport calculations.

The calculations show that the use of a windowed inner wall improves this chamber's response to photon sources by 17-300% over the energy range of 20-40 keV. Additionally, calculations show that for this chamber, the application of the standard temperature-pressure correction factor results in an over-correction of as much as 11-18% at air densities/pressures corresponding to 3048 m (10000 feet) for photon sources of 20-40 keV. Finally, comparing MCNP calculated responses as a function of air density to EGSnrc calculated responses show agreement to within 2.3% for photon sources of 20-40 keV.

We conclude that Monte Carlo transport calculations using MCNP accurately model the response of this well chamber. Additionally, we conclude that the use of a windowed inner wall is an effective feature for improving the chamber response to low energy photon sources. Finally, this work provides detailed Monte Carlo verification of the WC2 over-response effect when applying the standard temperature-pressure correction.

Key Words: brachytherapy, well-type ionization chamber

1 INTRODUCTION

Prostate cancer is the most common form of male cancer and is the second leading cause of male cancer deaths. There will be 230,110 new prostate cancer cases and 29,900 prostate cancer deaths in 2004 in the United States [1]. Permanent implantation of radioactive seeds directly into the prostate gland is an important treatment option for patients due to reduced complications compared to other treatment modalities. Additionally, several other cancers are commonly treated by temporarily or permanent implanting a radioactive source.

The goal in radiation therapy is to deliver a high radiation dose to the disease site while minimizing dose to healthy tissue. The technique of temporarily or permanently positioning small sealed radioactive sources directly into or near cancerous or other diseased sites is called *brachytherapy*. Because the radioactive sources are placed into or near the tumor, brachytherapy has the benefit of delivering high doses to the disease site while minimizing doses to surrounding healthy tissue.

In order to deliver an accurate treatment for the patient, the strength of these brachytherapy sources must be known to very precise standards. Measuring the source strength is performed by using a calibrated radiation detector (often an ionization chamber), to measure the output of the source. The measured strength of the source is then used by computerized treatment planning software to plan and deliver the radiation treatment to the patient. Thus it is vitally important to determine the strength of the source as accurately as possible.

Typically, well-type ionization chambers having calibrations traceable to national standards are used on site at therapy clinics to determine the strength of sources for quality assurance practices [2]. Well-type chambers are large ion chambers with a cylindrical shape and an opening to allow for insertion of the radioactive source. Because the gas filled active region almost completely surrounds the source, they produce a very efficient signal even for relatively weak sources. Two types of well chambers are currently used. The pressurized model in which the gas (often argon) is used to fill the active region of the well chamber and is pressurized to 1.5-20 atmospheres. The other type of chamber used is an air-communicating chamber where the gas in the active region of the chamber is air and is at the same pressure as the ambient atmosphere. The pressurized chamber has an advantage of a stronger signal since the gas is more dense, but these chambers often develop leaks over time. The air-communicating chamber has a weaker signal than the pressurized chamber but is not susceptible to leaking of the fill gas. These air-communicating well chambers are the most common type that are used in radiotherapy clinics.

In using a chamber open to atmospheric communication, a temperature and pressure correction is usually applied to account for the change of the air density in the collecting volume. [2, 3, 4] This correction for some pressure, P, and temperature, T in degrees Celsius, is given by

$$C_{TP} = \frac{(T + 273.15)}{(T_0 + 273.15)} \frac{P_0}{P}, \tag{1}$$

where P_0 is usually taken as 760 Torr and T_0 as 22^o C (hereafter referred to as the standard reference condition). The density for dry air at these conditions is $1.197\ kg/m^3$ and will be referred to as ρ_{STD} hereafter. [5]

In the atmosphere, air pressure decreases with elevation above the earth's surface since there is less air above a given surface at a high altitude compared to the amount of air above the same surface at sea level. It can be shown assuming constant temperature and constant gravitational force, that the air pressure falls exponentially with altitude above the earth's surface. The pressure P at height h is given by [6, 7]:

$$P = P_{\emptyset} e^{\frac{-Mgh}{RT}}, \tag{2}$$

where $P_{\emptyset}$ is the pressure at $h = 0$, M is the molecular mass of air, g is the gravitational acceleration, R is the universal gas constant, and T is the temperature in degrees Kelvin. Using

this equation, the air pressure at 1524 m (5000 feet) of elevation is about 84% of the pressure at sea level. Since pressure is directly proportional to density given a constant temperature, the density of the air at this elevation is also 84% of the air density at sea level. Often the approximation of a 1 in of Hg change in pressure per 1000 feet of elevation is used. Several large cities exist at higher elevations in North America, these include Albuquerque, NM (5311 feet), Calgary Canada (3540 feet), Denver, CO (5280 feet), and Salt Lake City, UT (4220 feet). [8]

Weather related changes in air density/pressure are significantly smaller than the elevation related changes. Typical weather effects are associated with changes in air pressure of $\pm 3\%$ during strong high pressure or deep low pressure systems and a strong hurricane can be associated with a 11% reduction in pressure. [8] These elevation and weather related differences in air pressure may be observed by examining the hourly weather station reporting data of the Denver/Boulder Colorado Office of the National Weather Service. [9] This compilation reports pressure data from stations with a wide range of elevations.

Recently, we have shown that the standard temperature-pressure correction used to account for changes in the response of well chambers open to atmospheric communication does not adequately describe the change in chamber response for low energy photon sources. [10] This is particularly evident when the chamber is used at higher elevations where the air pressure is substantially less than that at sea level. For the most commonly used well chamber (Standard Imaging HDR 1000 Plus), the application of the standard temperature-pressure correction can result in an over-response of 10% at air densities corresponding to elevations of 5000ft for a typical prostate brachytherapy seed. This 10% over-response can directly translate to a 10% under-dosage of the patient. Even at sea level elevations, there can be an over-response of 2% with the normal $\pm 3\%$ pressure changes associated with weather systems. A companion paper to our earlier work provides experimentally derived correction factors to aid clinicians in resolving this problem for some well chambers [11].

This work uses Monte Carlo transport calculations to analyze another well chamber open to atmospheric communication and used in the radiation therapy field, namely, the Precision Radiation Measurements model WC2 (formerly manufactured by PRM INC. Nashville,TN). This chamber is particularly interesting because it has a much larger active volume than the HDR 1000. Additionally, while our earlier work provided Monte Carlo based verification of measurements in the HDR 1000 Plus chamber, detailed Monte Carlo verification of the WC2 chamber was not performed.

1.1 Materials and Methods

1.1.1 Well Chamber Description

The WC2 chamber is an aluminum bodied cylindrical geometry well chamber approximately 150 mm in diameter and 340 mm high. The active volume is 2500 cm^3. The chamber is open to atmospheric communication. This is substantially larger than the 275 cm^3 active volume of the HDR 1000 Plus chamber examined in our earlier work. [10]. A schematic diagram of the chamber is shown in Figure 1. The important characteristics of the chamber are an aluminum alloy inner wall, an aluminum coated mylar covering the inner wall, an aluminum alloy collecting electrode, and an aluminum alloy body. The tube forming the inner wall has eight windows

(approximately 1 cm by 15 cm) machined out to allow low energy photon sources to produce a larger signal than would be possible with a solid inner wall.

Additionally, the air filled inner active region is 15.8 mm thick and the air filled outer active region is 28.0 mm thick. Note that this diagram is a simplified version of the actual detailed model used for calculations in this work as discussed below. For the work in this paper where a seed holder was included in the model, a custom machined acrylic single seed holder was modeled and consists of 2 support posts mounted on acrylic disks that fit into the chamber well. Two centrally located acrylic tube segments support teflon tubing that holds the seed in the center of the source holder.

1.1.2 Monte Carlo code and Library Description

MCNP is a Monte Carlo transport code system developed at Los Alamos National Laboratory. [12] MCNP is a generalized, continuous energy, three dimensional coupled neutron/photon/electron Monte Carlo transport code. MCNP traditionally uses a surface-sense geometry method where intersections and unions of first, second, and some fourth degree surfaces are used to define the problem geometry. Additionally, MCNP contains a macrobody capability which can further reduce the user effort required to model a complex geometry. MCNP's powerful geometry package is a strong advantage of this code system.

The calculations in this work were performed using MCNP version 4c3. The detailed photon physics option of MCNP was used in this work and includes treatment of coherent scattering, incoherent (Compton) scattering, photoelectric effect (with K and L shell fluorescence and Auger electron production following atomic relaxation) and pair production. Because the photoelectric cross sections for low Z materials used by some MCNP photon libraries are somewhat out of date [13], the fully updated library, *MCPLIB04* [14], was used. This library contains updated cross sections, form factors, scattering functions, and fluorescence data. The library is based on ENDF/B-VI release 8 whose cross sections are based on Lawrence Livermore National Laboratories EPDL-97. [15]

The electron transport method implemented in MCNP is a class I condensed history method with physics at the level of the Integrated Tiger Series (ITS) version 3. [12, 16] In MCNP, the condensed random walk for electron transport is based on energy steps (major steps). Pre-calculated and tabulated data for the electrons are saved on a predefined energy grid which corresponds to an average energy loss of 8.3% per major step. [12] The electron trajectory and production of secondary particles are controlled at the substep level. MCNP, like the ETRAN and ITS codes, uses the Goudsmit-Saunderson multiple scattering distribution to treat the angular deflection of the electron during its sub-step. MCNP and its associated cross section libraries can treat photon and electron transport down to 1 keV.

The EGSnrc code system is developed and maintained at the National Research Council of Canada (NRC) and is based on the EGS4 code system developed at Stanford Linear Accelerator Center (SLAC) and NRC. [18] EGSnrc is a three dimensional code package for coupled transport of both photons and electrons. The code package is a collection of subroutines and block data and, in general, requires a user written geometry and scoring routine. Well developed user codes are distributed with the code package that support generalized calculations in a three dimensional

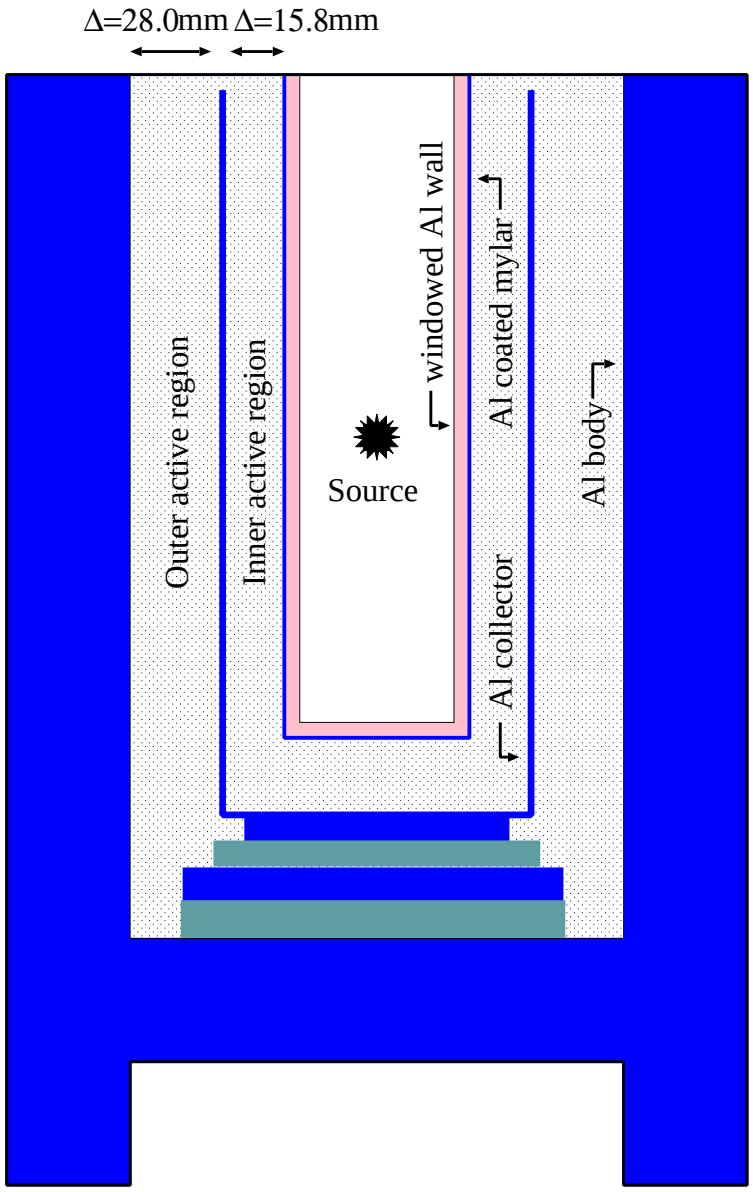

Figure 1: A simplified schematic diagram of the PRM WC2 well ionization chamber showing the source holder region, air filled active regions, collecting electrode and walls. The source holder is not shown for clarity.

R-Z geometry with azimuthal symmetry. For the work in this paper, the *dosrznrc* user code was run. EGSnrc's photon physics can treat coherent (Rayleigh) scattering, Compton scattering, pair production, and photoelectric effect (with K,L, and M shell fluorescent photon and Auger electron production following atomic excitation). [18] The standard photon cross section data distributed with EGSnrc is out of date, therefore the EGSnrc calculations performed for this work use an updated photon cross section library based on XCOM cross sections. [19, 20]

The EGSnrc code uses a class II condensed history method for electron transport. [17] In class II schemes inelastic collisions resulting in bremsstrahlung or delta particle emission above some threshold are treated explicitly. Below the threshold, processes are treated with a continuous slowing down model. Multiple elastic scattering is treated with an approximation to the Goudsmit-Saunderson theory. Near geometry boundaries, EGSnrc switches to single scattering mode to correctly model electron boundary crossings. The lack of correlation between energy loss and secondary particle production and the difficulties near boundaries when an electron step is interrupted can be a disadvantage of class I schemes.

In summary, it is generally agreed in the Medical Physics community that the treatment of electron physics in EGSnrc is better than MCNP, however the geometry package of MCNP is more powerful. MCNP is used for the primary analysis in this work and verification of MCNP results are implemented by comparison to EGSnrc calculations.

1.1.3 Calculation Description

A detailed model of the WC2 chamber was created from original engineering drawings and by partial disassembly and measurement of components from an existing chamber. Several photon sources were modeled in the chamber with the source holder including monoenergetic bare point sources of 10 keV to 600 keV. Additionally, detailed models of the Amersham 6711 ^{125}I based brachytherapy seed benchmarked in earlier work [13] were also used to examine the response of the well chamber. The decay spectrum for ^{125}I was taken from the National Nuclear Data Center's NuDat compilation. [21] All calculations were done transporting both photons and electrons.

The response of the chamber is determined using the energy deposited in the active region. This assumes that the charge collected is directly proportional to the charge produced in the chamber, and that the average energy expended to create an ion pair $(\bar{W}/e)$ is constant with particle speed. Energy deposition was tallied using a cell based energy balance scoring method (the *f8 tally in the MCNP code).

The chamber was modeled with an air density ranging from 70% of ρ_{STD} up to ρ_{STD}. From equation 2, these air densities correspond to elevations from 3048 m (10000 feet) down to sea level. For some photon energies, the air density range was expanded to include densities from 50%-200% of ρ_{STD}.

The number of particle histories used for calculations of energy deposition corresponded to statistical uncertainties (at the 1σ level) of on average 1.1% in the inner active region and 0.85% in the outer active region for the photon sources of 10-200 keV over the air density ranges investigated. Response calculations reported in this work used an electron cut-off energy of 5 keV for sources with energy 20 keV and higher and 2 keV for sources with energy below 20 keV.

1.2 Results

1.2.1 Response as a function of photon energy

Figure 2 shows the calculated response of the WC2 chamber with source holder to bare point monoenergetic photon sources ranging in energy from 10 keV to 200 keV. These responses are calculated with ρ_{STD}. In this plot the inner active region response, the outer active region response, and the total chamber response are shown. Notice the rise in the outer active region response as the photon energy increases from 10 to 20 keV. This is because as the photon energy increases from 10 to 20 keV, more photons are able to penetrate the collecting electrode and produce electrons in the outer active region. The response of the inner active region does not show a rise in this energy range because the windowed entrance wall allows the 10 keV photons to penetrate easily. Beyond about 20 keV, the response of both the inner and outer active region decreases as fewer photons are interacting in the chamber to produce electrons that ionize air in the active regions. Above 20 keV, the outer active region has a much larger response than the inner active region. This is because the outer active region has a much larger volume (1953 cm^3) compared to the inner active region (589 cm^3). Comparing the total response of the WC2 chamber

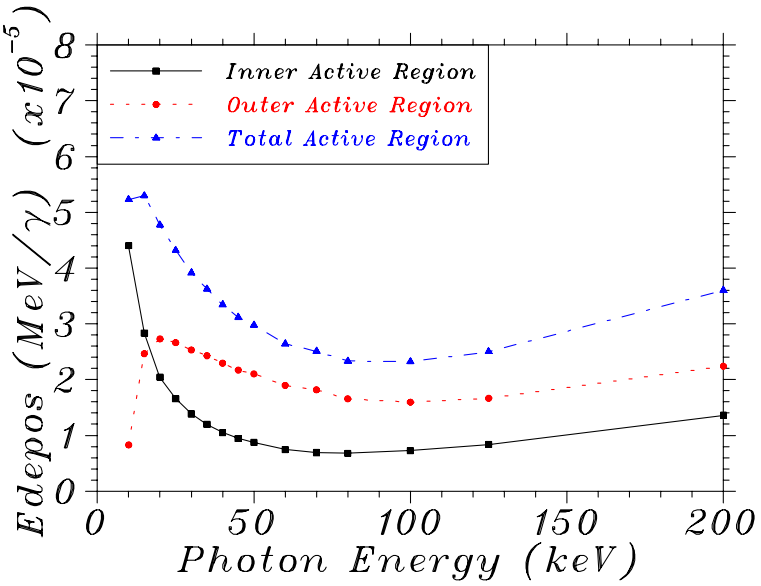

Figure 2: Calculated energy response of the WC2 well chamber to bare point photon sources.

to that of the HDR 1000 Plus examined in our earlier work (figure 2 of reference [10]), we see a much larger response in the WC2 chamber per starting photon. For example at 20 keV photon energy, the response of the WC2 chamber is 61% larger than the response of the HDR 1000 Plus. This is expected since the WC2 chamber has a much larger active region than HDR 1000 Plus.

Figure 3 shows the calculated response of the WC2 chamber with a hypothetical solid inner wall to bare point monoenergetic photon sources ranging in energy from 10 keV to 200 keV. Note how the solid inner entrance wall dramatically reduces the chamber response for photon energies below 40 keV. Since this well chamber is designed for low energy brachytherapy sources, the

designers chose to make the inner wall more transparent by machining eight windows into the tube forming the inner wall. The windowed wall increases the chamber response over a solid wall of the same thickness by 17-300% over the 20-40 keV energy range.

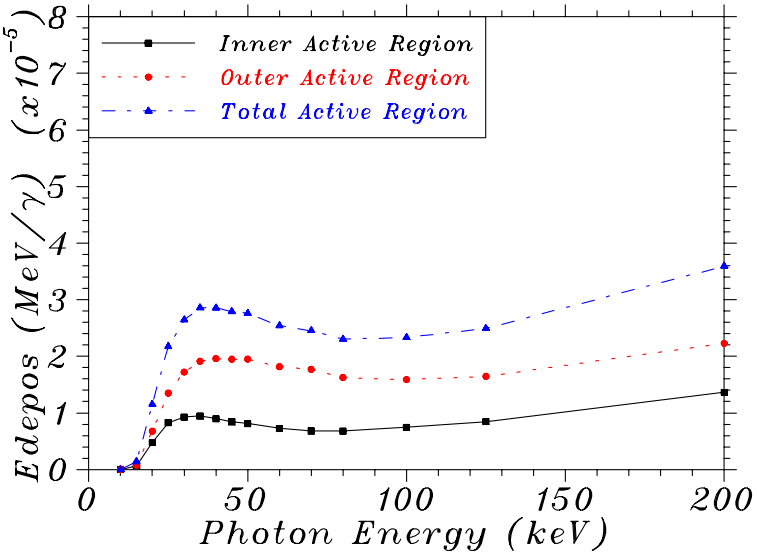

Figure 3: Calculated energy response of the WC2 well chamber with a solid entrance wall to bare point photon sources.

1.2.2 Response as a function of air density

Figure 4 shows the calculated response of the WC2 chamber with source holder as a function of air density to bare point monoenergetic photon sources of 20 keV to 100 keV. The calculated response is normalized to the response with ρ_{STD}. Note that this figure shows the raw response and does not include a C_{TP} factor. Figure 4 also includes the ratio of air density to ρ_{STD} as a function of air density. At lower photon energies, the response deviates significantly from the air density ratio. At higher photon energies, the response more closely follows that of the air density ratio. Elevation markings indicated on figures in this work are determined using equation 2 and the labels on the top x-axis are pressures corresponding to the air density assuming $T = 22^o\ C$.

Figure 5 shows the calculated C_{TP} corrected response normalized to the response with ρ_{STD}. Note the large deviation from unity of the normalized C_{TP} corrected response at low photon energies and low air densities (i.e. high elevations). From this figure, it is seen that the C_{TP} factor over-corrects the response of this chamber for low photon energies. For example, at an air density corresponding to 3048 m (10000 feet) in elevation for a photon source of 20 keV, the C_{TP} corrected response is about 11% larger than unity. At higher photon energies, the normalized C_{TP} corrected response is much closer to unity. As discussed in our earlier work, the reason this over-response effect occurs is because at lower photon energies, the range of the secondary electrons produced in the chamber walls and active region is often less than the distance across the active region of the chamber. The problem is made worse when the chamber walls are made of materials that backscatter a significant fraction of the incident electrons as the aluminum walls

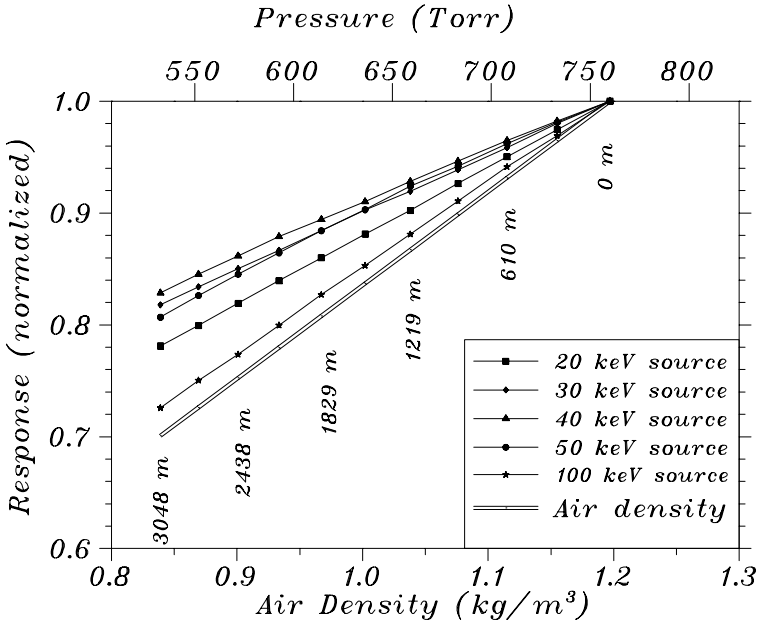

Figure 4: Calculated response of the WC2 chamber with source holder to monoenergetic bare point photon sources. Approximate elevation markings are shown and the top x-axis indicates air pressures at the given density assuming $T = 22^o\ C$**.**

do in the WC2 chamber. Further as discussed in our earlier work, the problem is that the C_{TP} correction factor is only appropriate for small ion chambers, it does not apply to medium size ion chambers. Here the size of an ion chamber is characterized in terms of the range of secondary electrons present in the active region.

It is interesting to compare the C_{TP} corrected response of this chamber to the HDR 1000 Plus chamber examined in our earlier work [10]. In the HDR 1000 Plus, the normalized C_{TP} corrected response at $\rho_{air} = 0.839\ kg/m^3$ decreased from 1.20 to 1.03 as the source energy increased from 20-100 keV. Note however that for the WC2 chamber, the normalized C_{TP} corrected response at $\rho_{air} = 0.839\ kg/m^3$ increases from 1.11 with a 20 keV photon source to 1.18 with a 40 keV photon source, and then decreases to 1.03 with a 100 keV photon source.

Figure 6 shows the calculated C_{TP} corrected response normalized to the response with ρ_{STD} for the model 6711 brachytherapy seed. This over-response is similar to that of a 30 keV bare point photon source. This is expected since the average emitted photon energy of a ^{125}I source is 28 keV. Note that at the air density/pressure corresponding to 1524 m (5000 feet) elevation, the C_{TP} corrected response is 7.5% higher than unity for the Amersham 6711 ^{125}I seed. From this plot one can see that even at sea level elevation, with the normal $\pm$3% pressure changes associated with weather systems, there can be an over-response of 1.5% for the Amersham 6711 ^{125}I seed. Comparing these results with the measurements presented by Griffin *et al.* [11] shows good agreement over the range of measurement (560-800 Torr). The maximum difference between the calculated and measured value for the normalized C_{TP} corrected response was 1.0%.

Figure 7 shows the C_{TP} corrected response normalized to the response with ρ_{STD} for a bare

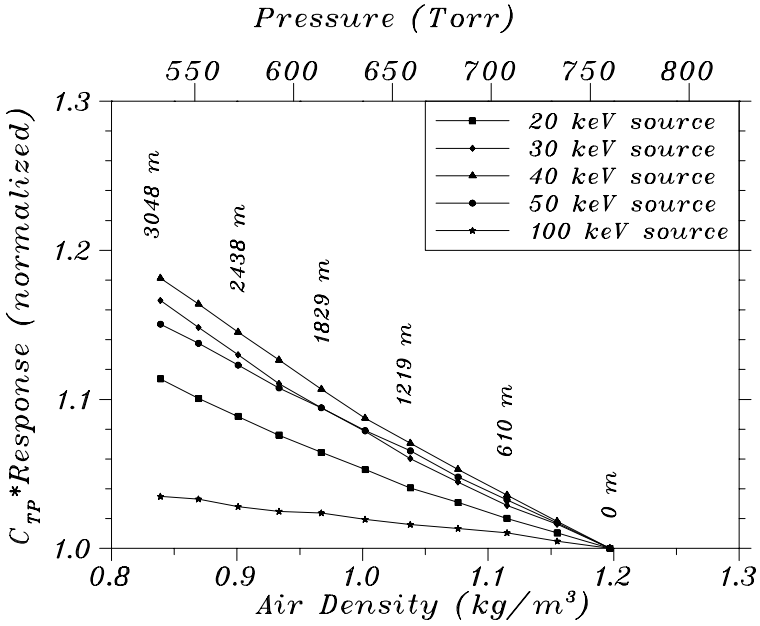

Figure 5: C_{TP} **corrected response of the WC2 chamber with source holder to monoenergetic bare point photon sources.**

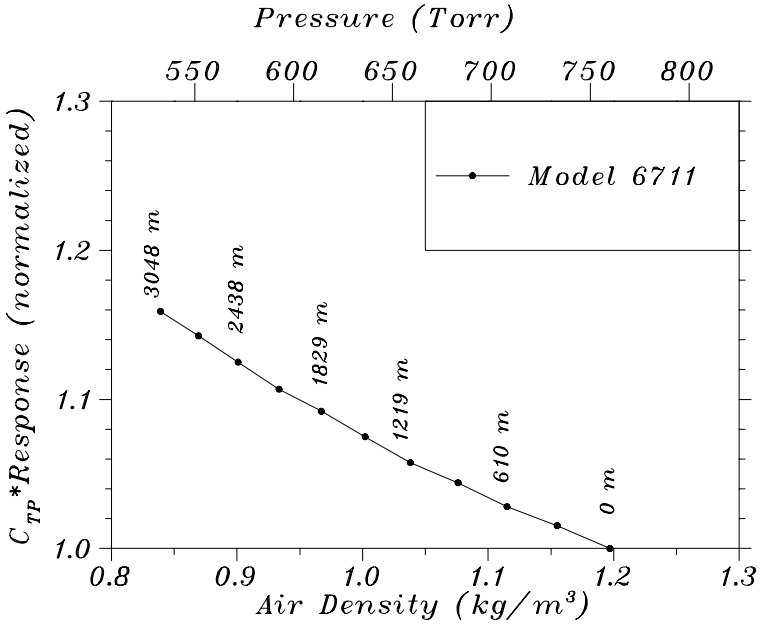

Figure 6: C_{TP} **corrected calculated response of the WC2 chamber with source holder to the Amersham 6711** ^{125}I **seed. Note that** C_{TP}***Response is normalized to the response with** ρ_{STD}**.**

point 20 keV photon source for a wide range of air densities. This figure clearly shows that the C_{TP} correction over-corrects for air densities less than ρ_{STD} and under-corrects for air densities greater than ρ_{STD}. Viewing the chamber response over this wide range of air densities shows non-linear behavior which can be difficult to discern over an air density range that may be encountered in clinics (e.g. figure 5). Additionally, figure 7 shows how the inner active region and outer active region behave differently. Applying the C_{TP} correction to the inner active region results in less of an over-response than applying the correction to the outer active region. This is because the distance across the inner active region (15.8mm) is less than the distance across the outer active region (28.0mm) and fewer of the secondary electrons are stopped in the inner active region.

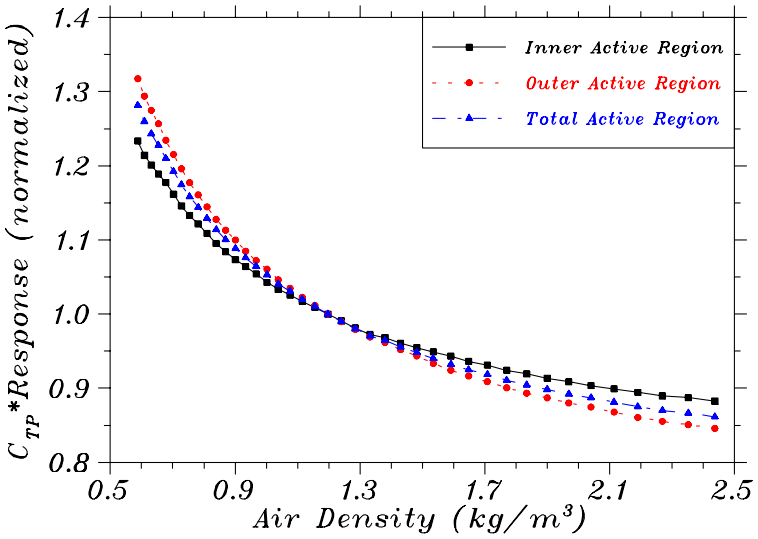

Figure 7: C_{TP} corrected calculated response of the WC2 well chamber with source holder to a 20 keV bare point photon source over a wide range of air densities.

1.2.3 Comparison to EGSnrc

In order to further verify that the MCNP code is accurately predicting the response of the WC2 well chamber, comparisons of the MCNP calculated response were made with the EGSnrc calculated response. Because the *dosrznrc* user code is limited to azimuthal symmetry, a model was created for *both* codes where no source holder was present and where the windowed entrance wall was replaced with a solid wall of reduced density. Bare point photon sources of 20-40 keV were investigated. For calculations of raw energy deposition in the active regions of the chamber, MCNP produced values 8% higher than EGSnrc. However in terms of the chamber response normalized to the response at ρ_{STD}, the agreement was very close with maximum differences of 2.3% or less observed over the 20-40 keV energy range investigated. Figure 8 shows the C_{TP} corrected response of the WC2 well chamber to a 30 keV bare point photon source as calculated with MCNP and EGSnrc.

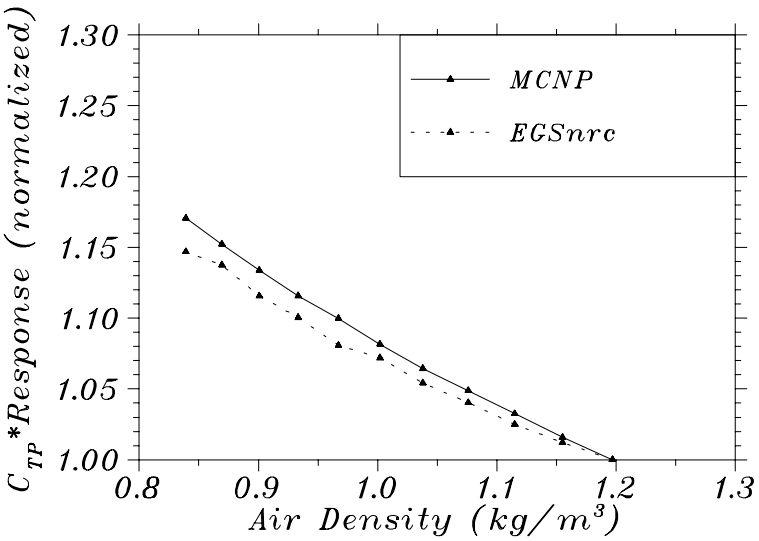

Figure 8: C_{TP} corrected response of the WC2 well chamber to a 30 keV bare point photon source as calculated with MCNP and EGSnrc.

2 CONCLUSIONS

In this paper we have used the MCNP Monte Carlo transport code to examine the response of the WC2 well chamber as both a function of photon source energy and air density. We have seen that because of the windowed inner wall design, this chamber has good sensitivity to low energy photons. We have also seen that the standard C_{TP} correction factor does not properly correct for the change in chamber response with low energy photon sources in this chamber. Finally, we have seen that the MCNP and EGSnrc codes produce good agreement in predicting the normalized response of the WC2 well chamber. Future work in this area may include the design of new well chamber not susceptible to the over-response effect.

3 ACKNOWLEDGMENTS

This work was partially supported by an Industrial and Economic Development Research (I&EDR) grant of the University of Wisconsin technology transfer program. Some of the calculations performed in this work used the National Science Foundation funded Grid Laboratory of Wisconsin (GLOW) computer cluster. Additionally, the authors would like to thank F. Hobeila and J. P. Seuntjens for providing the XCOM based photon cross section library for EGSnrc calculations.

4 REFERENCES

1. “Cancer Facts and Figures 2004” American Cancer Society.
2. R. Nath, L. L. Anderson, J. A. Meli, A. J. Olch, J. A. Stitt, and J. F. Williamson, “Code of practice for brachytherapy physics: Report of the AAPM Radiation Therapy Committee Task Group No. 56”, *Med. Phys.* **24**, pp. 1557-1598 (1997).

3. P. R. Almond, P. J. Biggs, B. M. Coursey, W. F. Hanson, M. Saiful Huq, R. Nath, and D. W. O. Rogers, "AAPM's TG-51 protocol for clinical reference dosimetry of high-energy photon and electron beams", *Med. Phys.* **26**, pp. 1847-1870 (1999).
4. L. A. DeWerd, "Brachytherapy Dosimetric Assessment: Source Calibration", in *RSNA Categorical Course in Brachytherapy Physics* edited by B. Thomadsen, (RSNA Publications, Oak Brook, IL, 1997), pp. 143-153.
5. R. C. Weast editor, *CRC handbook of Chemistry and Physics*, 58th Edition (CRC Press, West Palm Beach, FL, 1978).
6. M. N. Berberan-Santos, E. N. Bodunov, L. Pogliani, "On the barometric formula", Am. J. Phys. **65**, 404-412 (1997).
7. P. A. Tipler, *Physics*, 2nd edition (Worth Publishers, New York, NY, 1982).
8. C. D. Ahrens, *Meteorology Today*, 2nd edition (West Publishing, St. Paul, MN, 1985).
9. Current Conditions-Pressure Data, Denver/Boulder Office of the National Weather Service [online] http://www.crh.noaa.gov/den/awebshtml/webpres.shtml
10. T. D. Bohm, S. L. Griffin, P. M. DeLuca Jr., L. A. DeWerd, "The effect of ambient pressure on well chamber response: Monte Carlo calculated results for the HDR 1000 Plus", submitted to *Med. Phys.* June 2004.
11. S. L. Griffin, L. A. DeWerd, J. A. Micka, T. D. Bohm, "The effect of ambient pressure on well chamber response: Experimental results with empirical correction factors", submitted to *Med. Phys.* June 2004.
12. J. F. Briesmeister, Ed., "MCNP - A General Monte Carlo N-Particle Transport Code, Version 4C", Los Alamos National Laboratory report, LA-13709-M April, 2000.
13. T. D. Bohm, P. M. DeLuca Jr., L. A. DeWerd, "Brachytherapy dosimetry of ^{125}I and ^{103}Pd sources using an updated cross section library for the MCNP Monte Carlo transport code", *Med. Phys.* **30**, pp. 701-711 (2003).
14. M. C. White, "Photoatomic data library MCPLIB04: A new photoatomic library based on data from ENDF/B-VI Release 8", Los Alamos National Laboratory Memorandom, LA-UR-03-1019, February, 2003.
15. D.E. Cullen, J.H. Hubbell, L. Kissel, EPDL97: The Evaluated Photon Data Library, '97 Version, Lawrence Livermore National Laboratory report, UCRL-50400 Vol. 6, Rev. 5, September, 1997.
16. J.A. Halbleib, R.P. Kensek, T.A. Mehlhorn, G.D. Valdez, S.M. Seltzer, M.J. Berger, *ITS Version 3.0: The integrated TIGER series of coupled electron/photon monte carlo transport codes*, Sandia National Laboratories report, SAND91-1634, March 1992.
17. I. Kawrakow, "Accurate condensed history Monte Carlo simulation of electron transport. I. EGSnrc, the new EGS4 version", *Med. Phys.* **27**, pp. 485-498 (2000).
18. I. Kawrakow and D. W. O. Rogers, "The EGSnrc Code System: Monte Carlo Simulation of Electron and Photon Transport," National Research Council of Canada Report, PIRS-701, May 8, 2001.

19. M. J. Berger, J. H. Hubbell, S. M. Seltzer, J. S. Coursey, and D. S. Zucker, “XCOM: Photon Cross Section Database (version 1.2),” [Online] http://physics.nist.gov/xcom National Institute of Standards and Technology, Gaithersburg, MD (1999). Originally published as M. J. Berger and J. H. Hubbell, ”Photon Cross Sections on a Personal Computer,” NBSIR 87-3597; and as M. J. Berger and J. H. Hubbell, ”NIST X-ray and Gamma-ray Attenuation Coefficients and Cross Sections Database,” NIST Standard Reference Database 8, National Institute of Standards and Technology, Gaithersburg, MD (1987).
20. F. Hobeila, J. P. Seuntjens, “Effect of XCOM photoelectric cross-sections on dosimetric quantities calculated with EGSnrc”, IAEA-CN-96-17P+, Proceedings of the IAEA International Symposium on Standards and Codes of Practice in Medical Radiation Dosimetry Vienna, Austria, Nov. 25-28, 2002.
21. R. R. Kinsey, *et al.*, *The NUDAT/PCNUDAT Program for Nuclear Data*, 9th International Symposium of Capture Gamma-Ray Spectroscopy and Related Topics, Budapest, Hungary, October 1996. Data extracted from the NUDAT database, version 2.5, online at http://www.nndc.bnl.gov/